Complete Fragmentation Pattern for Two-Step Double Photoionization in Xenon

B. Kämmerling and V. Schmidt
Fakultät für Physik, Universität Freiburg, D-7800 Freiburg, Germany
(Received 15 July 1991)

An extensive study of the $4d_{5/2}$ photoionization in xenon is presented which allows, through the observation of the coincident N_5-$O_{23}O_{23}$ $^1S_0$ Auger electron, the establishment of the first complete fragmentation pattern for two-electron emission with information on the momenta and the spin projections of both electrons.

PACS numbers: 32.80.Fb, 32.80.Hd

If some external interaction causes a composite system to break up into its constituents, a typical fragmentation pattern arises. A simple case is given by single photoionization in free atoms where the breakup yields two particles only, the ion and the photoelectron. Because of the large mass of the atom (ion), the reference frame can be centered at the atom. Applying the dipole approximation and using linearly polarized light, the electric-field vector provides a convenient reference axis against which the fragmentation pattern can be described. In this case the pattern is determined by the observables of the emitted photoelectron, i.e., its momentum vector (including its energy value) and its spin polarization. While the measurement of the angular and energy distributions is common practice in photoionization studies, the fragmentation pattern including the spin requires angle-resolved spin-polarization measurements which are still rare due to experimental difficulties. Nevertheless, a detailed understanding can be achieved for this process [1]. In contrast, nothing is known about the complete fragmentation pattern for the case of two-electron emission where the momenta (including the energies) and the spin polarizations of both ejected electrons are connected and prevent a simple picture. Obviously, the study of such a fragmentation pattern requires a coincidence experiment. The first investigations of this challenging problem concentrated on direct double photoionization [2,3], where the energy and angle dependences of the fragmentation pattern were investigated. In this Letter we present the study of a specific two-step double photoionization process, $4d_{5/2}$ photoionization in xenon with a subsequent N_5-$O_{23}O_{23}$ $^1S_0$ Auger transition, where the presence of the Auger electron can be used to complete the information about the photoprocess such that the first fragmentation pattern for two-electron emission with information on the momenta and the spin projections of both coincident electrons can be established.

The experimental method is angle-resolved electron spectrometry [4] of the $4d_{5/2}$ photoelectron and the N_5-$O_{23}O_{23}$ $^1S_0$ Auger electron measured in coincidence. The experiment was performed at the electron storage ring BESSY in Berlin at the toroidal grating monochromator TGM5 of the undulator beam line. Proper tuning of the harmonics of the undulator light to 94.5-eV photon energy provided high photon flux and a high degree of linear polarization [Stokes parameters $S_1=0.957(5)$ and $S_2=0.0$]. A high linear polarization is important because the angular correlation between the photoelectron and the Auger electron depends also on the circularly polarized component of the incident light (Stokes parameter S_3) which cannot be determined directly at present. Coincidences between the $4d_{5/2}$ photoelectron and the N_5-$O_{23}O_{23}$ $^1S_0$ Auger electron were measured by placing the analyzer for the $4d_{5/2}$ photoelectron in a fixed position (azimuthal angle $\phi_1=150°$, polar angle $\Theta_1=90°$), but varying the position of the double-sector analyzer (ϕ_2 variable, $\Theta_2=90°$) which scans the N_5-$O_{23}O_{23}$ $^1S_0$ Auger line. The measured counting rate was corrected for the contribution of false coincidences, and the angle-dependent shift of the Auger line due to the post-collision interaction [5–7] was taken into account in the evaluation of true coincident intensities. The result is shown in Fig. 1 as points with error bars, and the solid line comes from a least-squares fit according to a theoretical relation (see below). Two interesting aspects of the observed angular distribution can be noted. First, neither the electric-field vector nor the direction of the photoelectron determines the symmetry. Second, at least two different loops appear which exhibit the presence of higher terms of the angular functions involved. Both aspects are comprised in the theoretical expression [8]

$$\frac{d^2\sigma}{d\Omega_1 d\Omega_2} = A_0 + A_2\cos2\phi_2 + B_2\sin2\phi_2 + A_4\cos4\phi_2 + B_4\sin4\phi_2 .$$

For a fixed direction of the emitted photoelectron, the coefficients A_i and B_i depend on the polarization of the incoming light and on the matrix elements describing the processes. The two-step formulation leads to a factorization for quantities belonging to the first and the second step, respectively. From the fitting procedure relative values for the coefficients are obtained (the finite size of the acceptance angles of the electron analyzers was taken into account).

The selected two-step process has the advantage that only one partial wave is possible for the emitted Auger electron. Hence, the numerical factors of the second step

are known and the ratios of the coefficients A_i/A_0 and B_i/A_0 depend in a nontrivial way on the photoprocess, and they provide four pieces of information. If this result is combined with our experimental data for the photoionization cross section, $\sigma(4d_{5/2})=12.2(1.5)$ Mb (cf. [9,10]), for the noncoincident angular distribution parameter of the photoelectron, $\beta(4d_{5/2})=0.35(1)$, and for the noncoincident alignment parameter, $\mathcal{A}_{20}(\frac{5}{2})=-0.230(15)$ (cf. [11]), the values of the dipole matrix elements together with their relative phases can be evaluated for all three photoionization channels. They are given by [for the definition of the matrix elements D_i see Ref. [12]; for the special case of $(LS)J$ coupling with only two matrix elements see Ref. [13]]

Channel		J	Matrix element
1	$4d_{5/2}^{-1}\epsilon p_{3/2}$	1	$D_1=d_1e^{i\Delta_1}$
2	$4d_{5/2}^{-1}\epsilon f_{5/2}$	1	$D_2=d_2e^{i\Delta_2}$
3	$4d_{5/2}^{-1}\epsilon f_{7/2}$	1	$D_3=d_3e^{i\Delta_3}$

with the following results at 94.5-eV photon energy:

$d_1=0.138(22)$ a.u.,

$d_2=-0.131(17)$ a.u., $\Delta_1-\Delta_2=3.04(10)$ rad, second solution with 3.24(10) rad,

$d_3=-0.474(59)$ a.u., $\Delta_2-\Delta_3=1.35(10)$ rad, second solution with $-1.35(10)$ rad.

Generally the relative phases occur in the equations for the observables as sine and cosine values, and both are needed in order to decide in which quadrant the desired phase difference lies. In the present case, the sine value is connected with the Stokes parameter S_3 which is unknown, too. Therefore, from the experimental data S_3 has to be determined also, but at the expense of a sign ambiguity for this quantity [$S_3=\pm0.17(5)$] and two solutions for the phase differences $\Delta_1-\Delta_2$ and $\Delta_2-\Delta_3$. Only two such phase differences are quoted, because $\Delta_1-\Delta_3$ simply follows from the other two, and the overall common phase is irrelevant. The established dipole matrix elements d_i and their relative phases represent a complete set for describing $4d_{5/2}$ photoionization in xenon at 94.5-eV photon energy [14].

Even though highly sophisticated calculations for $4d$ photoionization in xenon exist and lead to perfect agreement with the experimental data [cf. Refs. [15,16]; for relativistic RPA (RRPA) calculations cf. Refs. [17,18]], the possibility of deriving experimental values of dipole matrix elements was not considered, so that theoretical values for these quantities are not available at present [19]. If the experimental values of the above dipole matrix elements are used to calculate σ, β_{ph}, and $\mathcal{A}_{20}$, the experimental values are reproduced of course. In comparison to RRPA calculations [17], σ(theory) is considerably higher due to different relaxation processes not included in conventional RRPA. However, β_{ph}(theory) $=0.38$ is in good agreement with the experimental value. This has to be ascribed to the fact that this quantity contains the matrix elements in the numerator and denominator, thus eliminating a common scaling factor. The latter aspect is important also for the observables of spin polarization, where it follows that ξ(expt.) $=-0.70(16)$, η(expt.) $=\mp0.04(19)$, and ζ(expt.) $=-0.08(7)$ while the theory (adapted to the experimental binding energy) gives ξ(theory) $=-0.57$, η(theory) $=-0.18$, and ζ(theory) $=-0.26$.

On the basis of the experimental values for the dipole matrix elements, and taking advantage of the simplicity of the Auger transition with one partial wave only, we are able to proceed one step further and derive the complete fragmentation pattern for the coincident two-step electron-pair emission, including not only their momenta, but also their spin polarization. For this purpose, we have evaluated by the method of statistical tensor algebra the general expression for the fivefold differential cross section $d^5\sigma/d\Omega_1 d\Omega_2 dE\, d\mathbf{s}_1 d\mathbf{s}_2$ from which any desired information can be extracted. As an illustration we select

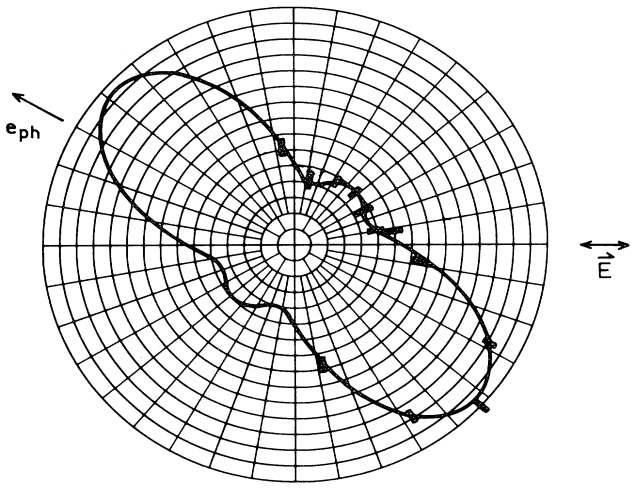

FIG. 1. Polar plot of coincident intensities between the $4d_{5/2}$ photoelectron and the N_5-$O_{23}O_{23}$ $^1S_0$ Auger electron in xenon. The photon beam passes the origin and is perpendicular to the plane of drawing; its main component of linear polarization (described by S_1) is indicated by **E**. the $4d_{5/2}$ photoelectrons are observed in the direction $\mathbf{e}_{ph}$. The intensities of true coincident N_5-$O_{23}O_{23}$ $^1S_0$ Auger electrons are given as points with error bars. The solid line represents the result of a least-squares fit according to the theoretical expression (see text).

the diametric emission of both electrons in a plane perpendicular to the photon beam and with an angle of 30° with respect to the electric-field vector. If the spin of the photoelectron is measured in the detector frame, the result for the spin-polarization vector of the Auger electron (in its own detector frame) can be predicted. This quantity is represented by the matrix $\mathbf{P}^{(2)}(\mathbf{s}_1,m_{s_1})$ which gives the Stokes parameter $\mathbf{P}^{(2)}$ for the spin of the Auger electron when the photoelectron's spin $\mathbf{s}_1$ is found to be m_{s_1} in a preselected direction $\mathbf{s}_1=(x_1,y_1,z_1)$. For the above geometry and 94.5-eV photon energy we obtain (note the two solutions for the relative phases)

$$\mathbf{P}^{(2)}(\mathbf{s}_1,m_{s_1})=\begin{pmatrix} P(x_2\uparrow-x_2\downarrow,x_1\uparrow) & P(y_2\uparrow-y_2\downarrow,x_1\uparrow) & P(z_2\uparrow-z_2\downarrow,x_1\uparrow)\\ P(x_2\uparrow-x_2\downarrow,x_1\downarrow) & P(y_2\uparrow-y_2\downarrow,x_1\downarrow) & P(z_2\uparrow-z_2\downarrow,x_1\downarrow)\\ P(x_2\uparrow-x_2\downarrow,y_1\uparrow) & P(y_2\uparrow-y_2\downarrow,y_1\uparrow) & P(z_2\uparrow-z_2\downarrow,y_1\uparrow)\\ P(x_2\uparrow-x_2\downarrow,y_1\downarrow) & P(y_2\uparrow-y_2\downarrow,y_1\downarrow) & P(z_2\uparrow-z_2\downarrow,y_1\downarrow)\\ P(x_2\uparrow-x_2\downarrow,z_1\uparrow) & P(y_2\uparrow-y_2\downarrow,z_1\uparrow) & P(z_2\uparrow-z_2\downarrow,z_1\uparrow)\\ P(x_2\uparrow-x_2\downarrow,z_1\downarrow) & P(y_2\uparrow-y_2\downarrow,z_1\downarrow) & P(z_2\uparrow-z_2\downarrow,z_1\downarrow) \end{pmatrix}$$

$$=\begin{pmatrix} -1.00 & 0.00 & 0.00\\ 1.00 & 0.00 & 0.00\\ -0.03 & 0.83 & 0.56\\ -0.03 & -0.83 & -0.56\\ -0.03 & -0.56 & 0.83\\ -0.03 & 0.56 & -0.83 \end{pmatrix} \text{ or } \begin{pmatrix} -1.00 & 0.00 & 0.00\\ 1.00 & 0.00 & 0.00\\ 0.03 & 0.83 & 0.56\\ 0.03 & -0.83 & -0.56\\ 0.03 & -0.56 & 0.83\\ 0.03 & 0.56 & -0.83 \end{pmatrix}$$

The first, third, and fifth rows of this matrix are presented graphically in Fig. 2 and allow the following interpretation: From part (a), if the x component of the photoelectron's spin (opposite to the photon beam) is measured, the spin-polarization vector of the Auger electron has a nonvanishing x component only in the opposite direction. This describes a singlet state for the total spin of the emitted electron pair, a situation which can be anticipated by the Russell-Saunders coupling scheme. However, relativistic effects can be expected for the heavy element xenon and, hence, contributions of triplet states. According to the couplings of angular momenta (p and f for the orbital angular momenta of the photoelectron and d of the Auger electron) and having $J=1$ for the total angular momentum of the electron-pair function, ${}^3P_1^\circ$ and ${}^3D_1^\circ$ states are possible in addition to ${}^1P_1^\circ$. As can be seen directly from parts (b) and (c) of Fig. 2, such contributions from triplet states are present, because the spin-polarization vector of the Auger electron is no longer opposite to the selected spin of the photoelectron. However, it should be kept in mind that details for the spin $\mathbf{S}$ of the electron-pair wave function cannot be extracted from the simple picture used to describe the complete fragmentation pattern of Fig. 2. For such studies the density matrix $[\rho(\mathbf{S},\mathbf{S}')]_{M_S,M_S'}$ must be worked out [20]. Nevertheless, the example provides a means of deriving information about the hitherto unknown two-electron continuum wave function from the complete fragmentation pattern of two-step double photoionization.

It is a pleasure for us to thank the members of BESSY for excellent research facilities. We are also thankful to B. Krässig for his help in setting up the experiment. The work has been funded by the German Federal Minister for Research and Technology (BMFT) under Contract

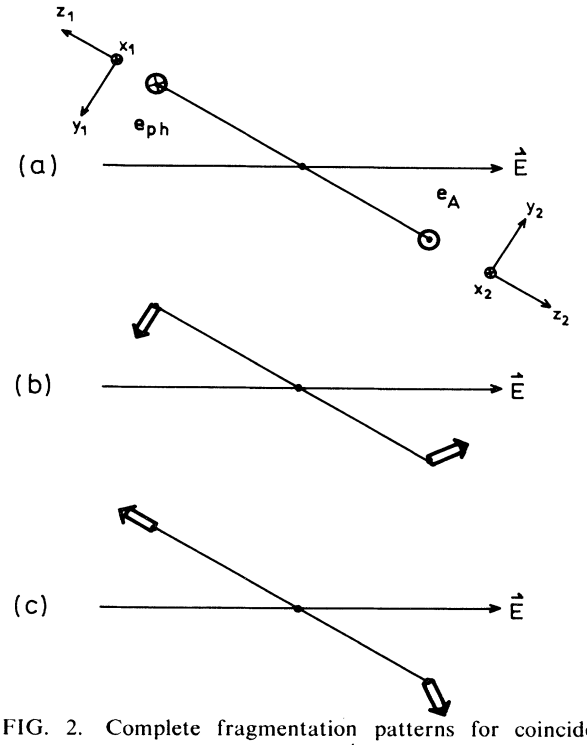

FIG. 2. Complete fragmentation patterns for coincident $4d_{5/2}$ photoelectron and N_5-$O_{23}O_{23}$ ${}^1S_0$ Auger electrons in a plane perpendicular to the photon beam (complete linear polarization with electric-field vector $\mathbf{E}$). The spin of the photoelectron (indicated by the open arrow) is preselected to lie (a) in the x_1 direction, (b) in the y_1 direction, and (c) in the z_1 direction; for the coincident Auger electron the associated spin-polarization vector $\mathbf{P}^{(2)}(\mathbf{s}_1,m_{s_1})$ is shown. The two solutions for the relative phases yield, for parts (b) and (c), a spin polarization of the Auger electron which points above and below the plane of drawing, respectively.

No. 054 72 AAI.

[1] U. Heinzmann, in *Proceedings of the International Conference on Vacuum Ultraviolet Radiation Physics, Lund, 1987,* edited by P. O. Nilsson and J. Nordgren [Phys. Scr. T **17** (1987)], and references therein.

[2] J. Mazeau, P. Selles, D. Waymel, and A. Heutz (to be published).

[3] V. Schmidt, in *Proceedings of the Fifteenth International Conference on X-Ray and Inner-Shell Processes, Knoxville, 1990,* edited by T. A. Carlson, M. O. Krause, and S. T. Manson, AIP Conf. Proc. No. 215 (AIP, New York, 1990), p. 559.

[4] H. Derenbach, Ch. Franke, R. Malutzki, A. Wachter, and V. Schmidt, Nucl. Instrum. Methods Phys. Res., Sect. A **260**, 258 (1987).

[5] M. Yu. Kuchiev and S. A. Sheinermann, Zh. Eksp. Teor. Fiz. **90**, 1646 (1986) [Sov. Phys. JETP **63**, 966 (1986)].

[6] J. Tulkki, G. B. Armen, T. Åberg, B. Crasemann, and M. H. Chen, Z. Phys. D **5**, 241 (1987).

[7] P. van der Straaten, R. Morgenstern, and A. Niehaus, Z. Phys. D **8**, 35 (1988).

[8] We are indebted to Dr. N. Kabachnik who made the general formula available to us prior to publication which corrects the treatment of S. C. McFarlane, J. Phys. B **8**, 895 (1975).

[9] B. Kämmerling, H. Kossmann, and V. Schmidt, J. Phys. B **22**, 841 (1989).

[10] U. Becker, D. Szostak, H. G. Kerkhoff, M. Kupsch, B. Langer, R. Wehlitz, A. Yagishita, and T. Hayaishi, Phys. Rev. A **39**, 3902 (1989).

[11] S. Southworth, U. Becker, C. M. Truesdale, P. H. Kobrin, D. W. Lindle, S. Owaki, and D. A. Shirley, Phys. Rev. A **28**, 261 (1983).

[12] K. N. Huang, Phys. Rev. A **22**, 223 (1980).

[13] A. Hausmann, B. Kämmerling, H. Kossmann, and V. Schmidt, Phys. Rev. Lett. **61**, 2669 (1988).

[14] There exist other possibilities to represent the content of a complete experiment, e.g., statistical tensors or density matrices for the photoionized state, J. Bohn and U. Fano, Phys. Rev. A **41**, 5953 (1990); X. C. Pan and A. Chakravorty, Phys. Rev. A **41**, 5962 (1990).

[15] Z. Altun, M. Kutzner, and H. P. Kelly, Phys. Rev. A **37**, 4671 (1988).

[16] M. Y. Amusia, L. V. Chernysheva, G. F. Gribakin, and K. L. Tsemekhman, J. Phys. B **23**, 393 (1990).

[17] K. N. Huang, W. R. Johnson, and K. T. Cheng, At. Data Nucl. Data Tables **26**, 33 (1981).

[18] M. Kutzner, V. Radojević, and H. P. Kelly, Phys. Rev. A **40**, 5052 (1989).

[19] M. Y. Amusia and H. P. Kelly (private communication).

[20] K. Blum, *Density Matrix Theory and Applications* (Plenum, New York, 1981).